

Symmetries and weak (anti)localization of Dirac fermions in HgTe quantum wells

P. M. Ostrovsky,^{1,2,3} I. V. Gornyi,^{2,4,5} and A. D. Mirlin^{2,6,5,7}

¹Max-Planck-Institut für Festkörperforschung, Heisenbergstr. 1, 70569, Stuttgart, Germany

²Institut für Nanotechnologie, Karlsruhe Institute of Technology, 76021 Karlsruhe, Germany

³L. D. Landau Institute for Theoretical Physics RAS, 119334 Moscow, Russia

⁴A.F. Ioffe Physico-Technical Institute, 194021 St. Petersburg, Russia.

⁵DFG Center for Functional Nanostructures, Karlsruhe Institute of Technology, 76128 Karlsruhe, Germany

⁶Inst. für Theorie der kondensierten Materie, Karlsruhe Institute of Technology, 76128 Karlsruhe, Germany

⁷Petersburg Nuclear Physics Institute, 188300 St. Petersburg, Russia.

We perform a symmetry analysis of a 2D electron system in HgTe/HgCdTe quantum wells in the situation when the chemical potential is outside of the gap, so that the bulk of the quantum well is conducting. In order to investigate quantum transport properties of the system, we explore symmetries of the low-energy Hamiltonian which is expressed in terms of two flavors of Dirac fermions, and physically important symmetry-breaking mechanisms. This allows us to predict emerging patterns of symmetry breaking that control the weak localization and antilocalization showing up in transverse-field magnetoresistance.

I. INTRODUCTION

Solid state systems with massless Dirac charge carriers have recently attracted an outstanding degree of attention of theoretical and experimental groups worldwide. This is mainly due to the impressive experimental progress in two physically related directions of research: graphene^{1,2} and topological insulators^{3,4}.

The notion of a topological insulator (TI) refers to a bulk insulator with gapless surface states occurring due to topological reasons. The simplest example of a topological insulator is the 2D electron gas in a strong magnetic field. At the quantum Hall plateau, the gap between Landau levels in the bulk is penetrated by a fixed integer number of chiral edge states providing the quantized value of the Hall conductance. The integer quantum Hall edge is thus a topologically protected 1D conductor realizing the group Z .

A novel class of TIs³⁻⁹ requires strong spin-orbit interaction in the absence of magnetic field (i.e. it is realized in systems with preserved time-reversal invariance). This type of TIs was discovered in HgTe/HgCdTe structures by the Würzburg group⁶. Strong spin-orbit interaction in HgTe leads to the inverted band gap in this semiconductor. As a result, the electron and hole bands are crossing near the boundary of the sample giving rise to the two counter-propagating helical edge modes. The time-reversal symmetry of the system leads to the topological protection of these edge modes.

Voltage applied to such a sample results in the appearance of the perpendicular spin current. This phenomenon is known as the quantum spin-Hall effect (QSHE). The robustness of the effect with respect to disorder makes it an extremely promising tool for applications. As a simplest example, the conversion between the usual charge current and spin current occurring in QSHE can be used for generation and detection of spin currents. The existence of a non-localized conducting channel at the edge of an (appropriately manufactured) two-dimensional HgTe/HgCdTe quantum well was experi-

mentally demonstrated in Refs. 6,10. These experiments, showing that HgTe/HgCdTe quantum wells provide a realization of a novel remarkable class of materials— Z_2 topological insulators—opened a new exciting research direction.

A 3D realization of a Z_2 TI was discovered in the experiment by Princeton group⁹ where crystals of $\text{Bi}_{1-x}\text{Sb}_x$ were studied (later other Bismuth compounds such as BiTe and BiSe were also shown to be 3D topological insulators). The 3D topological insulators exhibit very strong spin-orbit interaction also leading to the band gap inversion. This results in the appearance of gapless states on the surface of the sample forming a 2D topologically protected metal. The dynamics of the surface states is governed by the same massless Dirac Hamiltonian that has previously appeared in graphene. The main difference between graphene and the surface of a 3D topological insulator is the lack of the spin and valley degeneracy in the latter case. A combined effect of topology, disorder and interaction on a surface of 3D topological insulators was demonstrated to establish a novel critical 2D state with the low-temperature conductivity of order unity.¹¹

A similar critical state is expected¹¹ to separate the normal and topological insulator states in a 2D Z_2 topological insulators. In particular, such critical state should occur exactly at the QSHE transition in HgTe/HgCdTe quantum wells of critical thickness, when the 2D bulk gap is tuned to zero. The properties of this topologically protected metal reflect the quasirelativistic Dirac nature of carriers, similarly to the interference phenomena in graphene.^{22,23}

A two-dimensional metallic state in HgTe/HgCdTe quantum wells can also be realized in the presence of the bulk gap (either on the TI on the normal insulator side) by shifting the chemical potential (with a help of the gate) away from the gap. Such two-dimensional TI away from the TI regime represents a 2D spin-orbit metal, whose properties (in particular, interference corrections to the conductivity and low-field magnetoresistance) may still reflect the Dirac-fermion nature of car-

riers. In recent transport experiments the magnetoresistance of bulk-conducting HgTe/HgCdTe quantum wells was studied, both for inverted (thick wells)^{19–21} and normal (thin wells)^{20,21} band structures.

Although some aspects of the interference corrections in TI systems away from the TI regime have been already addressed theoretically¹⁴ there is a clear need in a systematic theory describing the whole variety of experimentally accessible regimes. The purpose of this paper is to develop such a theory. Analyzing the underlying Dirac-type Hamiltonian and physically relevant symmetry-breaking terms, we identify parameter regimes with different symmetries. The corresponding symmetry-breaking patterns determine the form of quantum interference magnetoresistance, i.e. the weak localization (WL) vs weak antilocalization (WAL) and corresponding prefactors.

The paper is organized as follows. In Sec. II we analyze symmetry properties of the Bernevig-Hughes-Zhang Hamiltonian and various physically relevant symmetry-breaking perturbations. This allows us to establish emerging patterns of symmetry breaking. In Sec. III we use these results to calculate the interference corrections (weak localization and weak antilocalization magnetoresistance) in various parts of the parameter space. Section IV contains a summary of our results and a brief comparison to available experimental data.

II. EFFECTIVE HAMILTONIAN AND SYMMETRIES

The standard approach to the description of electronic states in semiconductors is based on the $\mathbf{k} \cdot \mathbf{p}$ method. This method assumes that exact wave functions in the periodic potential of the crystal are known at some given point in the Brillouin zone. Normally, the states with zero quasimomentum (Γ point) are used. Then the effective Hamiltonian is constructed in the basis of these states by expansion in small momentum \mathbf{k} . The $\mathbf{k} \cdot \mathbf{p}$ perturbation theory thus provides the model Hamiltonian for the states close to the Γ point in terms of few matrix elements calculated with respect to exact eigenstates at $\mathbf{p} = 0$. The symmetries of the underlying system impose a number of constraints on the structure of the effective theory. In fact, a general form of the effective 2D Hamiltonian can be derived from the symmetry grounds, see Ref. 13, without invoking the microscopic (tight-binding or Kane-model) Hamiltonian.

The only intrinsic symmetry of the 3D Hamiltonian is time-reversal (TR): $H = s_y H^* s_y$. In the clean case, the point symmetry group is T_d (tetrahedral). Spatial inversion interchanges Hg and Te sublattices of the crystal. Neglecting the difference between Hg and Te, the point group becomes O_h (cubic). The approximate inversion symmetry leads to the block-diagonal structure of the BHZ Hamiltonian.

A. BHZ Hamiltonian

Effective Hamiltonian for a narrow symmetric HgTe quantum well (QW) was derived in Ref. 5 in the framework of the $\mathbf{k} \cdot \mathbf{p}$ method. The Bernevig-Hughes-Zhang (BHZ) Hamiltonian has a 4×4 matrix structure in the spin (sign of the z -projection of the total momentum \mathbf{J} , where the z -axis is perpendicular to the QW plane) and $E1 - H1$ space,

$$H_{\text{BHZ}} = \begin{pmatrix} h(\mathbf{k}) & 0 \\ 0 & h^*(-\mathbf{k}) \end{pmatrix}, \quad (1)$$

$$h(\mathbf{k}) = \begin{pmatrix} \epsilon(\mathbf{k}) + m(\mathbf{k}) & A(k_x + ik_y) \\ A(k_x - ik_y) & \epsilon(\mathbf{k}) - m(\mathbf{k}) \end{pmatrix}. \quad (2)$$

Here we have used the form given in Refs. 4,12,13 with the following arrangement of components in the spinor: $E1+$, $H1+$, $E1-$, $H1-$. Introducing the Pauli matrices $\sigma_{0,x,y,z}$ for the $E1-H1$ space and $s_{0,x,y,z}$ for the up-down (spin) space (with σ_0 and s_0 unity matrices), the effective Hamiltonian can be written as

$$H_{\text{BHZ}} = \epsilon(\mathbf{k})\sigma_0 s_0 + m(\mathbf{k})\sigma_z s_0 + Ak_x \sigma_x s_z - Ak_y \sigma_y s_0. \quad (3)$$

The functions $\epsilon(\mathbf{k})$ and $m(\mathbf{k})$ are effective energy and mass. Within the $\mathbf{k} \cdot \mathbf{p}$ expansion in the vicinity of the Γ point, they are

$$\epsilon(\mathbf{k}) = C + Dk^2, \quad m(\mathbf{k}) = M + Bk^2. \quad (4)$$

The two phases of normal and topological insulator correspond to $M > 0$ and $M < 0$, respectively. The sign of M changes at the critical thickness d_c of the QW of about 6.2 nm.⁶ Parameters A , B , and D are positive with $B > D$. The parameter C includes chemical potential and can be varied by changing the electron concentration with the gate voltage.

The Hamiltonian H_{BHZ} breaks up into two blocks acting independently in the spin-up and spin-down subspaces with the spectrum

$$E_{\pm}(\mathbf{k}) = \epsilon(\mathbf{k}) \pm \sqrt{A^2 k^2 + m^2(\mathbf{k})}. \quad (5)$$

The standard way¹⁴ to introduce disorder in the model is to add the fully diagonal term

$$H_{\text{dis}} = V(\mathbf{r})\sigma_0 s_0 \quad (6)$$

with a random potential $V(\mathbf{r})$ to the effective Hamiltonian H_{BHZ} . This corresponds to a relatively smooth (on the scale of the quantum well thickness) disorder. In particular, this model correctly describes charged impurities located at a certain (sufficiently large) distance R from the QW, e.g., in the doping layer. In this situation, within the QW the impurity potential is almost constant in z direction (across the QW), so that it does not break the $z \rightarrow -z$ symmetry of the QW. Alternatively, one can consider, e.g., placing short-range impurities exactly in the middle of the QW: such impurities would also preserve the $z \rightarrow -z$ symmetry and hence would not give rise to the mixing of the up and down blocks in H_{BHZ} .

In general, the Hamiltonian $H_{\text{BHZ}} + H_{\text{dis}}$ possesses two symmetries. Apart from the physical time-reversal symmetry $H(\mathbf{k}) = s_y H^*(-\mathbf{k}) s_y$, that relates the two spin blocks (Kramers doublets), the Hamiltonian commutes with s_z . This allows one to consider the two blocks separately. An extra symmetry can arise at some specific values of energy. In particular, $h(\mathbf{k})$ acquires its own time-reversal symmetry when the mass $m(k_F)$ is zero. This happens in the inverted regime ($M < 0$) when $M + Bk_F^2 = 0$.

It is also possible to achieve approximate orthogonal symmetry close to the bottom of the band, when $|M| \gg \{Ak_F, Bk_F^2\}$, and at very high energies $Bk_F^2 \gg \{|M|, Ak_F\}$. In the absence of block mixing, this would lead to WL. On the other hand, the regions of WL behavior at stronger magnetic fields (crossing over to WAL in weaker fields) were found in an experiment on similar structures^{19,20}, indicating that one can indeed achieve the regime of (approximate) orthogonal symmetry in this class of devices.

Thus we have identified three possible relevant symmetries of the model: physical time-reversal, spin, and block-wise time-reversal (either ‘‘symplectic’’ or ‘‘orthogonal’’). The latter symmetry can occur only in the presence of the spin symmetry, when the Hamiltonian breaks into two blocks. When all three symmetries are present, the two copies of symplectic or orthogonal class are realized leading to double WAL (i.e., with magnitude twice larger than the usual WAL correction) or double WL correction (with the same prefactor as in the conventional spinful orthogonal class). If the block-wise time-reversal symmetry is broken while spin symmetry is preserved, we obtain two copies of the unitary class with no interference corrections (in the lowest one-loop order). If the spin symmetry is also broken, the system realizes a single copy of symplectic class yielding the usual (not double) WAL correction. Finally, if the physical time-reversal symmetry is broken (e.g., by magnetic impurities), the single copy of unitary class is realized with no interference corrections (in the lowest order).

B. Symmetry breaking mechanisms in 2D

Let us list possible mechanisms of symmetry breaking in a 2D quantum well of HgTe.

Block-wise time-reversal symmetry is not exact from the very beginning. It is exact for massless Dirac fermions but is violated by the presence of $m(k) \neq 0$. In H_{BHZ} , this symmetry occurs only at one particular electron concentration. Since disorder mixes the states in the energy window of order $1/\tau$ near Fermi surface, it will inevitably break this symmetry. Another, and more relevant, possibility is the detuning of the average electron concentration from the point $M + Bk_F^2 = 0$.

Spin symmetry is broken by one of the following mechanisms:

(i) The block-diagonal structure of H_{BHZ} is not exact.

Off-diagonal elements in the effective Hamiltonian arise due to bulk inversion asymmetry (BIA) of the zinc-blende lattice of HgTe and have the form¹²

$$H_{\text{BIA}} = \begin{pmatrix} 0 & 0 & 2\delta_e k_+ & -\Delta_0 \\ 0 & 0 & \Delta_0 & 2\delta_h k_- \\ 2\delta_e k_- & \Delta_0 & 0 & 0 \\ -\Delta_0 & 2\delta_h k_+ & 0 & 0 \end{pmatrix} = \Delta_0 \sigma_y s_y + \delta_e (\sigma_0 + \sigma_z) (k_x s_x - k_y s_y) + \delta_h (\sigma_0 - \sigma_z) (k_x s_x + k_y s_y). \quad (7)$$

Here the first term with Δ_0 comes from the k_z^2 matrix elements connecting electrons from the Γ_6 band and heavy holes from the Γ_8 band that have opposite spins (such coupling is absent in a spherically symmetric Kane model in a bulk system).¹⁵ This term leads to the splitting of the spectrum into four branches:

$$E_{\pm}(\mathbf{k}) = \epsilon(\mathbf{k}) \pm \sqrt{(A|\mathbf{k}| \pm \Delta_0)^2 + m^2(\mathbf{k})}. \quad (8)$$

The linear-in- k terms with δ_e and δ_h arise after the projection of the bulk cubic Dresselhaus terms for electrons and holes, respectively, onto the QW. Typically, the spin-orbit interaction for holes is stronger than for electrons: $\delta_h \gg \delta_e$. The role of Dresselhaus-type terms increases with increasing k_F . These BIA mechanisms of breaking s_z symmetry are characterized by the corresponding symmetry breaking rates,

$$\frac{1}{\tau_{\Delta}} \sim \Delta_0^2 \tau, \quad (9)$$

$$\frac{1}{\tau_{\delta}^{e,h}} \sim (\delta_{e,h} k_F)^2 \tau, \quad (10)$$

within the Dyakonov-Perel spin relaxation mechanism (here τ is the transport scattering time due to disorder).

The BIA-induced terms are often neglected in the consideration of the quantum spin Hall effect in view of small coupling constants. Nevertheless, the break-down of the spin symmetry certainly occurs at sufficiently long scales (low temperatures), leading in the infrared limit to a single copy of a symplectic-class system (WAL without doubling).

(ii) Another way to break s_z symmetry is provided by the Rashba term arising in an asymmetric well (e.g., due to a finite gate voltage).^{12,13}

$$H_R = \begin{pmatrix} 0 & 0 & 2ir_0 k_- & 0 \\ 0 & 0 & 0 & 0 \\ -2ir_0 k_+ & 0 & 0 & 0 \\ 0 & 0 & 0 & 0 \end{pmatrix} = r_0 (\sigma_0 + \sigma_z) (-k_x s_y + k_y s_x). \quad (11)$$

Here we keep only the leading (linear-in- k) Rashba term connecting E1 up and E1 down subbands; other terms involving H1 bands are of higher order in k . Within the Dyakonov-Perel mechanism, the corresponding symmetry-breaking rate is

$$\frac{1}{\tau_R} \sim (r_0 k_F)^2 \tau, \quad (12)$$

(iii) The diagonal structure of H_{BHZ} is broken by atomically sharp impurities or interface roughness. This type of disorder, combined with the strong spin-orbit coupling in HgTe, leads to random non-diagonal terms in the Hamiltonian. Furthermore, the s_z symmetry can also be broken by finite-range (smooth on the lattice scale) impurities located in the quantum well. Such impurities break locally the $z \rightarrow -z$ symmetry of the QW and can be thought of as a kind of random Rashba term. Near the transition point, the leading (linear-in- k) contribution comes from the disorder-induced mixing of E1-up and E1-down blocks, similarly to the Rashba term. When disorder is created by distant charged impurities, such mixing is suppressed by an additional factor d/R , where d is the QW thickness and R is the spacer width.

C. Symmetry breaking mechanisms at the boundary

When the dephasing length L_ϕ is longer than one of the dimensions of a sample, the boundary conditions become important for the interference effects. This is, in particular, the case for universal conductance fluctuations in a coherent sample. Another example is the conductance of narrow stripes of HgTe in the regime $L_\phi \gg W$. While the width of the quantum well is of the order of few nanometers, its lateral width W can be restricted to about hundred nanometers. In such a restricted quasi-1D geometry, boundary conditions play a crucial role. Let us analyze the symmetries of the BHZ Hamiltonian with the boundary conditions.

We first assume that the boundary does not violate the spin symmetry and the Hamiltonian decomposes into two time reversed blocks $h(\mathbf{k})$ and $h^*(-\mathbf{k})$. Then the block-wise time reversal symmetry of $h(\mathbf{k})$ will be inevitably broken at the boundary. The easiest way to see this is to consider the Dirac limit of the Hamiltonian neglecting the mass in Eq. (3). Schrödinger equation with such a linear-in- k Hamiltonian is a system of two coupled linear first order differential equations. Boundary condition for such a system should be of the zero order in momentum, i.e., some linear constraint on the components of the wave function is imposed at the boundary. In a general form, we can write $b^T \psi = 0$ with some two component spinor b . The elements of b may depend on the conserved momentum parallel to the boundary. The time-reversal symmetry tells us that, if ψ is an eigenstate, then $s_y \psi^*$ is another eigenstate with the same energy. If boundary conditions preserve this symmetry then the latter eigenfunction would obey $b^T s_y \psi^* = 0$. Equivalently, $b^\dagger s_y \psi = 0$. Thus we have two linear conditions on ψ instead of one. These conditions are consistent only if the vectors b and $s_y b^*$ are linearly related: $b = a s_y b^*$ with some constant a . Multiplying the last expression by b^\dagger from the left, we obtain $b^\dagger b = a b^\dagger s_y b^* = a \text{tr}(s_y b^* b^\dagger)$. The left-hand side is strictly positive while the right-hand side contains a trace of the product of antisymmetric (s_y)

and symmetric ($b^\dagger b^*$) matrices and is hence zero. This apparent controversy proves that any boundary conditions for a single copy of massless Dirac Hamiltonian will inevitably break its time-reversal invariance.

The simplest way to see this is as follows: in order to produce a “wall” for a single Dirac-fermion species, one has to open a gap by switching on a big mass near the boundary, which breaks the effective time reversal symmetry already after a single boundary scattering event. This fact is well known in the context of graphene studies, where in the absence of the intervalley scattering it is impossible to confine Dirac quasiparticles without opening the gap at the boundary.

An alternative boundary condition $\psi = 0$ for the BHZ Hamiltonian is widely used in literature. In order to apply this boundary condition, the quadratic terms in the Hamiltonian should be retained. The relation $\psi = 0$ is invariant under time-reversal transformation. Nevertheless, the time-reversal symmetry is broken at the boundary even in this case. A detailed proof of the symmetry breaking is relegated to Appendix A.

We thus conclude that the block-wise symplectic time-reversal symmetry is always broken near the boundary. In particular, in a quasi-1D system the corresponding symmetry-breaking rate is given by

$$\frac{1}{\tau_{\text{edge}}} \sim \frac{D}{W^2}, \quad (13)$$

where W is the stripe width. This τ_{edge} is just the average time for an electron to diffuse across the system and get aware of the boundary conditions.

When the block-wise time-reversal symmetry is of the orthogonal type (e.g., when the Fermi energy is located near the bottom of the spectrum), the boundary condition $\psi = 0$ does not introduce additional symmetry breaking, in contrast to the “Dirac case”. Indeed, the system belonging to the conventional orthogonal class can be confined by large potential. Then the “relativistic corrections” would interplay with the boundary scattering just in the same way as with the impurity scattering.

So far, we have considered the boundary conditions preserving the spin symmetry. The spin symmetry may be broken by the edges of a 2D sample if the edges are not ideal in z -direction. This situation, which can be modeled by short-range impurities located near the boundaries, seems to be quite likely in a realistic setup. In this case the only remaining symmetry is the physical (symplectic) time-reversal symmetry.

III. INTERFERENCE CORRECTIONS FROM SYMMETRY CONSIDERATION

In this section we describe the general symmetry-based formalism for calculating the interference corrections in an infinite 2D sample. We closely follow the approach¹⁶ developed for Dirac fermions in a disordered graphene (see also Ref. 22).

Quite generally, the existence of a singular (logarithmic in T or B) conductivity correction is related to the presence of a certain time-reversal (TR) symmetry that acts on an operator \mathcal{O} according to

$$T: \mathcal{O} \mapsto U^{-1} \mathcal{O}^T U, \quad (14)$$

where U is some unitary operator (note that the momentum operator changes sign under transposition). For the 4×4 matrix Hamiltonian one can introduce 16 possible TR symmetries

$$T_{ij}: \mathcal{O} \mapsto \sigma_i s_j \mathcal{O}^T s_j \sigma_i, \quad (15)$$

that would correspond to 16 soft modes (Cooperons). For example, the Hamiltonian $H_{2\mathcal{O}} = [\epsilon(k) + V(\mathbf{r})] \sigma_0 s_0$ (physically, this Hamiltonian corresponds to spinful electrons in two valleys of a normal metal, without any spin and valley mixing effects) is invariant under all these 16 symmetries. This gives rise to 16 logarithmic corrections to the conductivity of the form

$$\delta\sigma_{ij} = -c_{ij} \frac{e^2}{2\pi h} \ln\left(\frac{\tau_\phi}{\tau}\right), \quad c_{ij} = \pm 1. \quad (16)$$

The sign factors c_{ij} here are determined by the sign of the time-reversal operator squared $T^2 = \pm 1$. In the present case we have $T_{ij}^2 = (\sigma_i s_j)(\sigma_i s_j)^*$. In particular,

$$\sigma_0 s_0 (\sigma_0 s_0)^* = 1 \implies T_{00}^2 = 1, \quad (17)$$

$$\sigma_y s_0 (\sigma_y s_0)^* = -1 \implies T_{y0}^2 = -1, \quad (18)$$

$$\sigma_y s_y (\sigma_y s_y)^* = 1 \implies T_{yy}^2 = 1, \quad (19)$$

and so on. One can see that out of 16 TR symmetries only 6 (namely, T_{0y} , T_{xy} , T_{y0} , T_{yx} , T_{yz} , T_{zy}) contribute with the minus sign, yielding for $H_{2\mathcal{O}}$ the total conductivity correction

$$\delta\sigma = -(-6 + 10) \frac{e^2}{2\pi h} \ln\left(\frac{\tau_\phi}{\tau}\right) = -2 \times \frac{e^2}{\pi h} \ln\left(\frac{\tau_\phi}{\tau}\right). \quad (20)$$

This is the WL correction for two independent copies of orthogonal symmetry class.

In general, not all the possible TR symmetries are respected by the dominant term in the Hamiltonian. Therefore, as a first step in calculating the logarithmic correction one should retain only the TR symmetries of the dominant term, setting all other $c_{ij} = 0$. The sub-leading terms in the Hamiltonian may further break the remaining TR symmetries on the scale τ_{sb} , introducing gaps in the soft modes and thus cutting off the logarithmic terms by τ_{sb} . As a result, in the low- T limit, the singular term $\ln(\tau_\phi/\tau)$ remains only for those TR symmetries that are preserved by all terms in the Hamiltonian. With increasing T , τ_ϕ becomes shorter than the symmetry breaking time τ_{sb} and the system crosses over to another symmetry class.

A. Weak antilocalization in HgTe quantum wells:

$$E_F \gg m(k_F)$$

Let us now return to the case of HgTe and employ this machinery to it. In order to directly use the results of Ref. 16, we interchange E1 and H1 states in the spin-up block. In this basis (H1+, E1+, E1-, H1-), the BHZ Hamiltonian (2) takes the form:

$$H_{BHZ} = \epsilon(\mathbf{k}) \sigma_0 s_0 + [-m(\mathbf{k}) \sigma_z + A \mathbf{k} \boldsymbol{\sigma}] s_z. \quad (21)$$

The linear-in- k (massless Dirac) term in this 4×4 Hamiltonian has the same structure as in Ref. 16 (there the matrices τ_i corresponding to two graphene valleys played a role of s_i here).

We will now consider the situation when this term in the Hamiltonian is dominant, i.e. when the Fermi energy $E_F \gg m(k_F)$ is in the range of almost linear spectrum $E_\pm \simeq \pm A|k|$, so that the mass term as well as the spin-symmetry breaking terms can be considered as perturbations. In this representation, the s_z -symmetry breaking terms read:

$$H_{BIA} = \Delta_0 \sigma_z s_x + \delta_+ (k_x \sigma_x + k_y \sigma_y) s_x \quad (22)$$

$$+ \delta_- (k_x \sigma_y - k_y \sigma_x) s_y, \quad (23)$$

$$H_R = r_0 [(k_x \sigma_y + k_y \sigma_x) s_x - (k_x \sigma_x - k_y \sigma_y) s_y], \quad (24)$$

where $\delta_\pm = \delta_h \pm \delta_e$.

The massless Dirac Hamiltonian (“graphene Hamiltonian”)

$$H_A = A(k_x \sigma_x + k_y \sigma_y) s_z \quad (25)$$

is invariant under the following four TR symmetries:

$$T_{xx}: \mathcal{O} \mapsto \sigma_x s_x \mathcal{O}^T \sigma_x s_x, \quad T_{xx}^2 = 1, \quad (26)$$

$$T_{y0}: \mathcal{O} \mapsto \sigma_y s_0 \mathcal{O}^T \sigma_y s_0, \quad T_{y0}^2 = -1, \quad (27)$$

$$T_{yz}: \mathcal{O} \mapsto \sigma_y s_z \mathcal{O}^T \sigma_y s_z, \quad T_{yz}^2 = -1, \quad (28)$$

$$T_{xy}: \mathcal{O} \mapsto \sigma_x s_y \mathcal{O}^T \sigma_x s_y, \quad T_{xy}^2 = -1, \quad (29)$$

which in Ref. 16 were denoted as T_0, T_x, T_y, T_z , respectively. As a result, the conductivity correction for two independent copies of massless Dirac fermions is positive:

$$\delta\sigma = -(1 - 3) \frac{e^2}{2\pi h} \ln\left(\frac{\tau_\phi}{\tau}\right) = 2 \times \frac{e^2}{2\pi h} \ln\left(\frac{\tau_\phi}{\tau}\right), \quad (30)$$

which is a doubled WAL (two copies of symplectic class).

Let us now take into account the mass term $H_M = -m(\mathbf{k}) \sigma_z s_z$ in H_{BHZ} . This term is invariant under T_{xx} and T_{xy} while breaking down T_{y0} and T_{yz} . The corresponding symmetry breaking rate $1/\tau_m$ was calculated in Ref. 14. The conductivity correction in this case can

be written as

$$\begin{aligned} \delta\sigma &= \frac{e^2}{2\pi h} \left[\ln \frac{\tau}{\tau_\phi} - \ln \left(\frac{\tau}{\tau_\phi} + \frac{\tau}{\tau_m} \right) \right. \\ &\quad \left. - \ln \left(\frac{\tau}{\tau_\phi} + \frac{\tau}{\tau_m} \right) - \ln \frac{\tau}{\tau_\phi} \right] \\ &= -2 \times \frac{e^2}{2\pi h} \ln \left(\frac{\tau}{\tau_\phi} + \frac{\tau}{\tau_m} \right). \end{aligned} \quad (31)$$

At lowest T , when $\tau_\phi \gg \tau_m$, we have

$$\delta\sigma \simeq 2 \times \frac{e^2}{2\pi h} \ln \left(\frac{\tau_m}{\tau} \right), \quad (32)$$

which is not singular in T . This corresponds to two copies of a unitary class. With increasing T the symmetry-breaking term $1/\tau_m$ becomes unimportant and the system crosses over to two copies of symplectic class, Eq. (30).

So far, we have considered the block-diagonal s_z -symmetric Hamiltonian H_{BHZ} . Let us now take into account the inversion-asymmetry terms H_{BIA} and H_R . The main difference between HgTe and graphene is the structure of such symmetry breaking terms. The inter-valley disorder scattering in graphene preserves only T_{xx} symmetry. As a result, when the valley mixing is strong, the quantum correction to the conductivity is negative (WL): graphene with mixed valleys belongs to the orthogonal symmetry class. In contrast, the mixing of the up/down blocks in HgTe QWs involves an additional spin structure which generically kills the orthogonal T_{xx} symmetry. Generically, the only remaining TR symmetry is the symplectic T_{xy} symmetry surviving the SO interaction. Therefore, at lowest temperatures the HgTe QW is expected to be a single copy of a symplectic system with ordinary WAL.

The k -independent term $\Delta_0 \sigma_z s_x$ in H_{BIA} violates T_{xx} and T_{y0} , while preserving T_{yz} and T_{xy} . This leads to

$$\begin{aligned} \delta\sigma &= \frac{e^2}{2\pi h} \left[\ln \left(\frac{\tau}{\tau_\phi} + \frac{\tau}{\tau_\Delta} \right) - \ln \left(\frac{\tau}{\tau_\phi} + \frac{\tau}{\tau_m} + \frac{\tau}{\tau_\Delta} \right) \right. \\ &\quad \left. - \ln \left(\frac{\tau}{\tau_\phi} + \frac{\tau}{\tau_m} \right) - \ln \frac{\tau}{\tau_\phi} \right]. \end{aligned} \quad (33)$$

Two situations are possible: (i) $\tau_\Delta \gg \tau_m$ and (ii) $\tau_\Delta \ll \tau_m$. Starting at high T , with lowering T in case (i) the system first crosses over from two copies of symplectic class, Eq. (30), to two copies of unitary class, Eq. (32), and then at $\tau_\phi \sim \tau_\Delta$ to a single copy of a symplectic class with ordinary WAL:

$$\delta\sigma = \frac{e^2}{2\pi h} \ln \left(\frac{\tau_\phi}{\tau} \right). \quad (34)$$

We denote such an evolution as $2\text{Sp} \rightarrow 2\text{U} \rightarrow 1\text{Sp}$. In case (ii), for $\tau_\Delta \ll \tau_\phi$ we get

$$\delta\sigma \simeq \frac{e^2}{2\pi h} \left[-\ln \left(\frac{\tau}{\tau_\phi} + \frac{\tau}{\tau_m} \right) - \ln \frac{\tau}{\tau_\phi} \right]. \quad (35)$$

which corresponds to the crossover $2\text{Sp} \rightarrow 1\text{Sp}$ at $\tau_\phi \sim \tau_m$ ($2\text{WAL} \rightarrow 1\text{WAL}$). Note that at $\tau_\phi \sim \tau_\Delta$ the number of soft modes does not change, despite the transitions between the spin blocks.

Finally, in the presence of Dresselhaus and/or Rashba terms, the only effective TR symmetry is T_{xy} . The effect of short-range impurities within the QW is similar to that of the Rashba term. Denoting the total symmetry-breaking rate due to such terms as $1/\tau_{\text{SO}}$, we get (here neglecting the Δ_0 -term):

$$\begin{aligned} \delta\sigma &= \frac{e^2}{2\pi h} \left[\ln \left(\frac{\tau}{\tau_\phi} + \frac{\tau}{\tau_{\text{SO}}} \right) \right. \\ &\quad \left. - 2 \ln \left(\frac{\tau}{\tau_\phi} + \frac{\tau}{\tau_m} + \frac{\tau}{\tau_{\text{SO}}} \right) - \ln \frac{\tau}{\tau_\phi} \right]. \end{aligned} \quad (36)$$

Again, for $\tau_m \ll \tau_{\text{SO}}$, we have $2\text{Sp} \rightarrow 2\text{U} \rightarrow 1\text{Sp}$, whereas for $\tau_m \gg \tau_{\text{SO}}$ the mass term is not important ($2\text{Sp} \rightarrow 1\text{Sp}$).

The general formula for the conductivity correction at $E_F \gg m(k_F)$ including all symmetry-breaking terms combines Eqs. (33) and (36):

$$\begin{aligned} \delta\sigma &= \frac{e^2}{2\pi h} \left[\ln \left(\frac{\tau}{\tau_\phi} + \frac{\tau}{\tau_\Delta} + \frac{\tau}{\tau_{\text{SO}}} \right) \right. \\ &\quad \left. - \ln \left(\frac{\tau}{\tau_\phi} + \frac{\tau}{\tau_m} + \frac{\tau}{\tau_\Delta} + \frac{\tau}{\tau_{\text{SO}}} \right) \right. \\ &\quad \left. - \ln \left(\frac{\tau}{\tau_\phi} + \frac{\tau}{\tau_m} + \frac{\tau}{\tau_{\text{SO}}} \right) - \ln \frac{\tau}{\tau_\phi} \right]. \end{aligned} \quad (37)$$

Here $1/\tau_\phi$ is the dephasing rate due to inelastic processes, τ is elastic transport scattering time, τ_Δ was defined in Eq. (9), $1/\tau_{\text{SO}}$ is the total spin-orbit rate describing the combined effect of Dresselhaus and Rashba terms, Eqs. (10) and (12) (as well as the SO impurity scattering), $1/\tau_m$ is the rate of breaking effective time-reversal symmetry within each spin block due to finite mass of Dirac fermions. This mechanism of symmetry breaking is analogous to the one in the case of interplay between Rashba and Zeeman splitting: the Rashba term tends to fix the spin direction in the 2D plane according to the momentum of a particle, whereas the Zeeman field tends to align the spin in the direction of magnetic field (out of the 2D plane). Without impurity scattering, each state is characterized by a certain direction of spin. The symmetry-breaking rate can be estimated using an analogy with the Dyakonov-Perel mechanism, $\tau_m^{-1} \sim \Delta_m^2 \tau$, where effective spin-precession frequency Δ_m is only non-zero in the presence of disorder:

$$\Delta_m \propto \frac{m(k_F)}{Ak_F} \frac{1}{\tau}, \quad (38)$$

which yields

$$\frac{1}{\tau_m} \sim \frac{1}{\tau} \left[\frac{m(k_F)}{E_F} \right]^2 \quad (39)$$

in the regime of interest. A rigorous calculation of a Cooperon¹⁷ (which can be simplified by dressing the impurity potential by Dirac factors, thus reducing the problem to a spinless one in the presence of a peculiar disorder potential) confirms this estimate. This result agrees with Ref. 14 in this limit.

Assuming for simplicity an energy-independent disorder scattering rate (which, in fact, is generically not the case for Dirac particles, see, e.g., Ref. 16), we can express the symmetry-breaking length $l_m = (D\tau_m)^{1/2}$ in terms of the carrier density n :

$$l_m \propto \frac{A}{\left| \pm \frac{|M|}{\sqrt{n}} + B\sqrt{n} \right|}, \quad (40)$$

where the sign \pm distinguishes between the inverted ($-$) and normal ($+$) band structures.

We have identified the only true soft mode (corresponding to the true Kramers TR symmetry), which governs the localization properties at lowest temperatures. It gives rise to a single WAL correction (single symplectic class: 1Sp). This is not surprising, as the symplectic TR symmetry is the only true TR symmetry in a system with strong spin-orbit interaction. On the other hand, on short time scales (equivalently, high temperatures) the symmetry may be higher if the corresponding symmetry-breaking terms are not yet operative. Depending on the values of symmetry-breaking rates, there may be different patterns of symmetry breaking:

- (i) 2Sp \rightarrow 2U \rightarrow 1Sp. This first scenario is realized when the mass term in H_{BHZ} is more important than the s_z -symmetry-breaking terms: $\tau \ll \tau_m \ll \min[\tau_\Delta, \tau_{SO}]$. In this case, at high temperatures the system behaves as two copies of symplectic class (2Sp) with doubled WAL. In the intermediate range of temperatures $\tau_m \ll \tau_\phi \ll \min[\tau_\Delta, \tau_{SO}]$, the system behaves as two copies of unitary class (2U) with no T -dependent interference correction. Finally, at $\tau_\phi \gg \min[\tau_\Delta, \tau_{SO}]$ the two spin blocks are completely mixed and the system reaches its generic spin-orbit state 1Sp (single copy of symplectic class with ordinary WAL).
- (ii) 2Sp \rightarrow 1Sp. This scenario is realized in the case of the following hierarchy of scales: $\tau \ll \min[\tau_\Delta, \tau_{SO}] \ll \tau_m$, when the block mixing is faster than the breaking of the effective TR symmetry within each block. As a result, there is no room for the unitary class in this case.
- (iii) 1Sp. When the complete mixing of spin blocks is very fast, which happens when $\tau_{SO} \lesssim \tau$ or $\max[\tau_m, \tau_\Delta] \lesssim \tau$, the system behaves as a single copy of symplectic class (1Sp) in the whole diffusive regime (ordinary WAL).

Let us estimate which of these scenarios can be expected in experiments on HgTe QWs. According to Table I of Ref. 4, the value of the BIA-induced splitting

Δ_0 in HgTe QW near the QSHE transition is $\Delta_0 \simeq 0.0015 - 0.002\text{eV} \sim 15 - 20K$. When the 2D mean free path is $0.1 - 0.5\mu\text{m}$, one finds (using $A \simeq 3.65 - 3.9\text{ eV \AA}$)

$$\Delta_0\tau \simeq 0.5 - 2.5 \sim 1. \quad (41)$$

This implies that for such values of the mean free path there is no room for scenario (i). The conductivity correction for $\Delta_0\tau \gtrsim 1$ has the form

$$\delta\sigma \simeq \frac{e^2}{2\pi h} \left[-\ln \left(\frac{\tau}{\tau_\phi} + \frac{\tau}{\tau_m} + \frac{\tau}{\tau_{SO}} \right) - \ln \frac{\tau}{\tau_\phi} \right]. \quad (42)$$

Then for $\min[\tau_m, \tau_{SO}] \gg \tau$ the pattern (ii) 2Sp \rightarrow 1Sp is realized, while for $\min[\tau_m, \tau_{SO}] \lesssim \tau$ there is single copy of symplectic system (1Sp) in the diffusive regime.

In a perpendicular magnetic field, a magnetoresistance arises due to the suppression of the interference correction by magnetic field. In the diffusive regime $L_\phi, L_H \gg l$ [where $L_H = (\hbar c/eB)^{1/2}$ is the magnetic length and l is the mean free path], the effect of magnetic field can be described by the replacement

$$\frac{1}{\tau_\phi} \rightarrow \frac{1}{\tau_\phi} + \frac{D}{L_H^2} \quad (43)$$

in the above zero- B formulas (here D is the diffusion coefficient). A more accurate expression (valid also in the limit of weak magnetic field, $D\tau_\phi/L_H^2 \ll 1$) has the standard Hikami-Larkin-Nagaoka¹⁸ form with digamma functions replacing logarithms. For a single copy of symplectic system, Eq. (34), the magnetoconductivity $\Delta\sigma(B) = \sigma(B) - \sigma(0)$ has the form

$$\begin{aligned} \Delta\sigma(B) &= -\frac{e^2}{2\pi h} \mathcal{H} \left(\frac{\tau}{\tau_\phi}, \frac{B}{B_{tr}} \right), \\ \mathcal{H}(x, y) &= \psi \left(\frac{1}{2} + \frac{x}{y} \right) - \psi \left(\frac{1}{2} + \frac{1}{y} \right) - \ln x, \end{aligned} \quad (44)$$

where $B_{tr} = \hbar/(2el_{tr}^2)$ is the value of magnetic field for which L_H is equal to the transport mean-free path l_{tr} and $\psi(x)$ is a digamma function. When the zero- B expression contains a combination of several logarithms representing the contributions of various channels, in the formula for the magnetoconductivity, each of logarithms is to be replaced according to Eq. (44), with $1/\tau_\phi \rightarrow 1/\tau_\phi + 1/\tau_{sb}$, where $1/\tau_{sb}$ is the total symmetry breaking rate for given channel. Weak antilocalization leads then to a positive magnetoresistance.

Importantly, in the regime $E_F \gg m(k_F)$ considered above there is no room for weak localization behavior which would manifest itself as a negative magnetoresistance. However, in Refs. 19,20 a crossover from positive to negative magnetoresistance was observed with increasing magnetic field in samples with not too high carrier densities. Such a crossover is characteristic to conventional spin-orbit systems with $\tau_{SO} \gg \tau$. In order to describe this behavior in HgTe quantum wells we have to consider the opposite limit $E_F \ll m(k_F)$, where the off-diagonal ("spin-orbit") terms in the Hamiltonian can be considered as a small perturbation.

B. Weak localization in HgTe quantum wells:

$$E_F \ll m(k_F)$$

Let us now consider the limit of low densities, when the Fermi energy is smaller than m . This is the limit of the conventional Schrödinger equation in the relativistic Dirac description. In this case, the spectrum can be expanded in A^2k^2 (for definiteness, we consider the upper branch):

$$E_+(\mathbf{k}) = \epsilon(\mathbf{k}) + \sqrt{A^2k^2 + m^2(\mathbf{k})} \\ \simeq |M| + Bk^2 + \epsilon(\mathbf{k}) + \frac{A^2k^2}{|M|}. \quad (45)$$

In this case the pseudospin is almost fixed along the z -direction by the “Zeeman field” M , while the off-diagonal terms in the Hamiltonian can be viewed as a weak “relativistic” correction (analogous to spin-orbit coupling), see Appendix B. On short scales the system is therefore close to the orthogonal symmetry class and should exhibit negative magnetoresistance in sufficiently strong magnetic field.

As discussed above, a similar situation is possible for the BHZ Hamiltonian at very high densities, when $Bk_F^2 \gg \{|M|, Ak_F\}$, where the spectrum is given by

$$E_+(\mathbf{k}) \simeq Bk^2 + \epsilon(\mathbf{k}) + M + \frac{A^2}{B}. \quad (46)$$

However, in realistic systems, when the first term in the small- k expansion becomes dominant, the expansion is expected to break down: all higher-order terms are expected to be as relevant as the lowest-order one (Bk^2 here). The analysis of the system at such high energies requires a more detailed knowledge of the spectrum. Therefore, here we will focus on the controllable case of small energies.

Now we consider the massless Dirac Hamiltonian $H_A = A(k_x\sigma_x + k_y\sigma_y)s_z$ as a perturbation to the diagonal part of the BHZ Hamiltonian

$$H_M = -m(\mathbf{k})\sigma_z s_z, \quad (47)$$

dominated by the mass term $m(\mathbf{k}) = M + Bk^2$. The Hamiltonian (47) is invariant under the following eight TR symmetries:

$$T_{00} : \mathcal{O} \mapsto \sigma_0 s_0 \mathcal{O}^T \sigma_0 s_0, \quad T_{00}^2 = 1, \quad (48)$$

$$T_{0z} : \mathcal{O} \mapsto \sigma_0 s_z \mathcal{O}^T \sigma_0 s_z, \quad T_{0z}^2 = 1, \quad (49)$$

$$T_{xx} : \mathcal{O} \mapsto \sigma_x s_x \mathcal{O}^T \sigma_x s_x, \quad T_{xx}^2 = 1, \quad (50)$$

$$T_{xy} : \mathcal{O} \mapsto \sigma_x s_y \mathcal{O}^T \sigma_x s_y, \quad T_{xy}^2 = -1, \quad (51)$$

$$T_{yx} : \mathcal{O} \mapsto \sigma_y s_x \mathcal{O}^T \sigma_y s_x, \quad T_{yx}^2 = -1, \quad (52)$$

$$T_{yy} : \mathcal{O} \mapsto \sigma_y s_y \mathcal{O}^T \sigma_y s_y, \quad T_{yy}^2 = 1, \quad (53)$$

$$T_{z0} : \mathcal{O} \mapsto \sigma_z s_0 \mathcal{O}^T \sigma_z s_0, \quad T_{z0}^2 = 1, \quad (54)$$

$$T_{zz} : \mathcal{O} \mapsto \sigma_z s_z \mathcal{O}^T \sigma_z s_z, \quad T_{zz}^2 = 1. \quad (55)$$

We see that there are overall six symmetries of the “orthogonal” type (yielding WL) and two “symplectic” (yielding WAL). However, we have to take into account that the Hamiltonian H_M breaks into blocks corresponding to positive and negative energies (conduction band and valence band). The two blocks correspond to eigenvalues of $\sigma_z s_z$ equal to ± 1 . The transport is determined only by one of these blocks (where the Fermi energy is located).

Therefore, eight symmetries Eqs. (48) – (55) split in four pairs,

$$\begin{aligned} T_{00} &\sim T_{zz}, \\ T_{0z} &\sim T_{z0}, \\ T_{xx} &\sim T_{yy}, \\ T_{xy} &\sim T_{yx}, \end{aligned} \quad (56)$$

and each pair should be counted only once for the calculation of the WL correction since two symmetries of the pair become identical when reduced to any of two $\sigma_z s_z$ eigenblocks. This yields

$$\delta\sigma = -(3-1)\frac{e^2}{2\pi h} \ln\left(\frac{\tau_\phi}{\tau}\right) = -\frac{e^2}{\pi h} \ln\left(\frac{\tau_\phi}{\tau}\right), \quad (57)$$

that is the contribution of an antilocalizing singlet and a localizing triplet. This is a conductivity correction for two independent copies of orthogonal symmetry class.

Let us now include the off-diagonal Dirac term $H_A = A(k_x\sigma_x + k_y\sigma_y)s_z$. The Hamiltonian $H_M + H_A$ still separates into two blocks with approximate orthogonal symmetry but positive- and negative-energy sectors are now mixed. Effective Hamiltonian valid near the Fermi energy is derived in Appendix B. Breaking of the time-reversal symmetry within a single block of the BHZ Hamiltonian can be traced back to the appearance of an effective magnetic field [with the vector potential given by Eq. (B7)] due to the interplay of “relativistic corrections” and disorder scattering. The weak localization correction (57) is modified by the presence of this effective magnetic field,

$$\delta\sigma = \frac{e^2}{\pi h} \ln\left(\frac{\tau}{\tau_A} + \frac{\tau}{\tau_\phi}\right), \quad (58)$$

where $1/\tau_A$ is the symmetry-breaking rate due to H_A (it is analogous to $1/\tau_M$ introduced above). The value of $1/\tau_A$ can be estimated as follows. Adding disorder potential to H_{BHZ} , we project the full Hamiltonian on a single chiral branch. The off-diagonal part H_A would lead to the appearance of the “spin-orbit” impurity scattering characterized by

$$\Delta_A \sim \frac{1}{\tau} \frac{A^2 k_F^2}{m^2(k_F)}. \quad (59)$$

This estimate yields

$$\frac{1}{\tau_A} \sim \Delta_A^2 \tau \sim \frac{1}{\tau} \left[\frac{Ak_F}{m(k_F)} \right]^4. \quad (60)$$

Alternatively, using the reduced spinless Hamiltonian (B8), one can evaluate the averaged phase difference S_a (“dephasing action”) accumulated due to the effective vector potential, Eq. (B7), on the time-reversed paths within the path-integral formalism (for definiteness, we consider the case when the Fermi level is located near the bottom of the spectrum, $E_F \ll |M|$):

$$\begin{aligned} S_a &\sim e^2 \left\langle \int d\mathbf{l}_1 \mathbf{a}(\mathbf{r}_1) \int d\mathbf{l}_2 \mathbf{a}(\mathbf{r}_2) \right\rangle_{\text{dis}} \\ &\sim \frac{1}{M^2} \left\langle \int d\mathbf{l}_1 \times \nabla V(\mathbf{r}_1) \int d\mathbf{l}_2 \times \nabla V(\mathbf{r}_2) \right\rangle_{\text{dis}}. \end{aligned} \quad (61)$$

Using the short-range correlated potential,

$$\langle V(\mathbf{r}_1)V(\mathbf{r}_2) \rangle_{\text{dis}} = \frac{\delta(\mathbf{r}_1 - \mathbf{r}_2)}{2\pi\nu\tau},$$

one can estimate

$$S_a \sim \frac{v_F k_F^3}{M^2 \nu \tau} t, \quad (62)$$

where $\nu \sim |M|/A^2$ is the density of states, $v_F = k_F A^2/|M|$ is the Fermi velocity, and all the gradients, as well as the inverse size of impurity, are replaced by k_F . From $S_a \sim 1$ we find $t \sim M^2 \nu \tau / v_F k_F^3$, which yields Eq. (60). Again, the derivation¹⁷ of a Cooperon within the kinetic equation approach and diagrammatics confirms this estimate.

The scaling of the corresponding symmetry-breaking length $l_A = (D\tau_A)^{1/2}$ with the carrier concentration n for energy-independent τ has the form:

$$l_A \propto \left(\pm \frac{|M|}{\sqrt{n}} + B\sqrt{n} \right)^2. \quad (63)$$

It is interesting to note that there is a formal relation between the symmetry-breaking lengths in the symplectic [Eq. (40)] and orthogonal [Eq. (63)] cases:

$$\frac{l_m}{l} = \sqrt{\frac{l}{l_A}}. \quad (64)$$

In each of the cases only one length is relevant, whereas the other is then shorter than the mean free path, implying no diffusive dynamics in the corresponding channel. Both lengths become of the order of the mean free path for $E_F \sim m(k_F)$, where without valley mixing the logarithmic first-order interference correction does not develop at all (2U phase).

Let us now include BHZ block-mixing rates τ_Δ^{-1} and τ_{SO}^{-1} . As we have pointed out above, the eight symmetries (48) – (55) of the Hamiltonian H_M split into four pairs (56). The symmetries within each pair are indistinguishable near the Fermi energy. The general rule for the evaluation of the WL correction is as follows. For each of the pairs (56), one of the following three situations is

possible: (i) Both symmetries from the pair are preserved (which means that the system splits into two eigenblocks of $\sigma_z s_z$). Then the pair contribute to the WL correction as a single time-reversal symmetry. (ii) One of two symmetries is broken, the other one is preserved. Then the situation becomes conventional, and the remaining mode gives a usual logarithmic contribution. (iii) Both symmetries from the pair are broken. Clearly, there is no contribution from this pair to the WL (WAL) correction in this case. To summarize, the pair gives a contribution as a single Cooperon mode, unless both symmetries are broken. The fact that one should break both symmetries to suppress the contribution implies that one should add symmetry-breaking times (rather than rates) corresponding to both symmetries of a pair and then invert the result in order to get the mass of the corresponding mode.

In our case additional terms have the following symmetries. The Dirac kinetic term H_A preserves only T_{xx} and T_{xy} out of the list (48)–(55). The Δ -term $H_\Delta = \Delta_0 \sigma_z s_x$ conserves T_{00} , T_{z0} , T_{xy} , and T_{yy} . The Rashba and Dresselhaus terms (linear in momentum) conserve T_{xy} and T_{yx} . This yields the following result for the WL correction:²⁴

$$\begin{aligned} \delta\sigma &= \frac{e^2}{2\pi h} \left[2 \ln \left(\frac{\tau}{\tau_\phi} + \frac{\tau}{\tau_A} + \frac{\tau}{\tau_{SO}} \right) \right. \\ &\quad \left. + \ln \left(\frac{\tau}{\tau_\phi} + \frac{\tau}{\tau_{SO}} + \frac{\tau}{\tau_A + \tau_\Delta} \right) - \ln \frac{\tau}{\tau_\phi} \right]. \end{aligned} \quad (65)$$

The only massless mode here again corresponds to the T_{xy} symmetry (physical symplectic TR symmetry). Thus in the presence of all block-mixing terms, the system becomes a single copy of the symplectic class. Depending on the relation between τ_A^{-1} , τ_Δ^{-1} , and τ_{SO}^{-1} , three patterns of symmetry breaking are possible:

- (i) $2O \rightarrow 2U \rightarrow 1Sp$. This scenario is realized when $\tau \ll \tau_A \ll \min[\tau_\Delta, \tau_{SO}]$. In this case, at high temperatures the system behaves as two copies of orthogonal class (2O) with doubled WL. In the intermediate range of temperatures $\tau_A \ll \tau_\phi \ll \min[\tau_\Delta, \tau_{SO}]$, the system behaves as two copies of unitary class (2U) with no T -dependent interference correction. Finally, at $\tau_\phi \gg \min[\tau_\Delta, \tau_{SO}]$ the two spin blocks are completely mixed and the system reaches its generic spin-orbit state 1Sp (single copy of symplectic class with ordinary WAL).
- (ii) $2O \rightarrow 1Sp$. This scenario is realized when $\min[\tau_\Delta, \tau_{SO}] \ll \tau_A$ and $\tau \ll \min[\tau_A, \tau_{SO}]$, i.e., when the block mixing is faster than the breaking of the effective orthogonal TR symmetry within each block. As a result, there is no room for the unitary class in this case.
- (iii) 1Sp. When the complete mixing of spin blocks is very fast, which happens when $\tau_{SO} \lesssim \tau$, the system

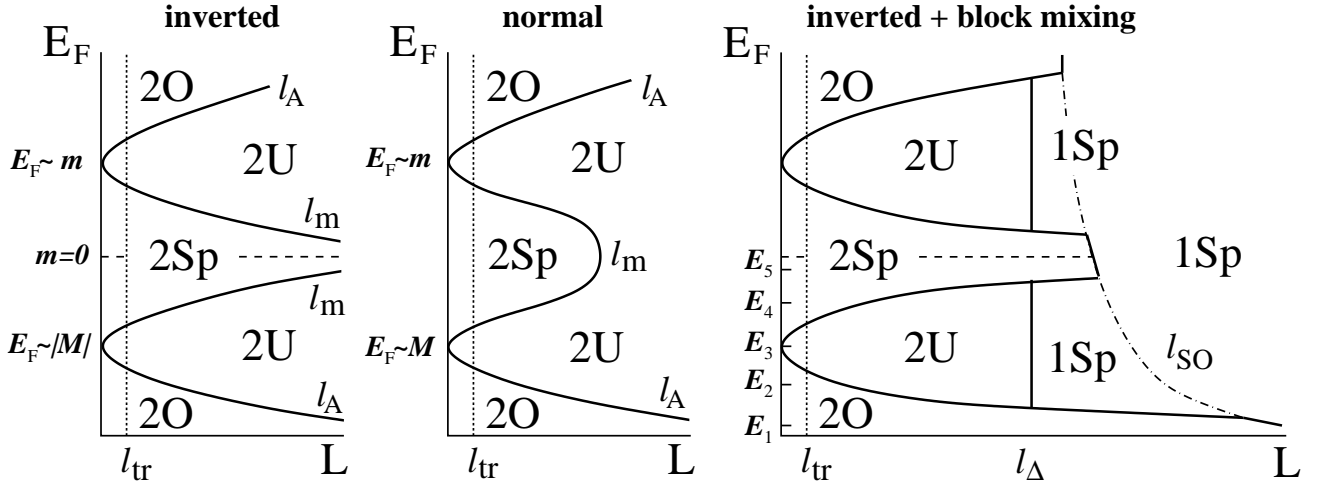


FIG. 1: Schematic diagram showing the symmetry patterns in the $L - E_F$ plane. Here L is the system size, phase-breaking length L_ϕ , or magnetic length L_H , whichever is shorter. For simplicity, the transport scattering length l_{tr} (vertical dotted line) is assumed to be energy independent (this assumption does not affect the “topology” of the diagram). The “phase boundaries” are shown by solid curves. Boundaries of the 2U-regions are determined by $l_m = (D\tau_m)^{1/2}$ for 2Sp \rightarrow 2U crossover, and by $l_A = (D\tau_A)^{1/2}$ for 2O \rightarrow 2U crossover. *Left panel:* Inverted band structure (thick quantum well) with no block mixing. Dashed line shows energy for which $m(k_F) = -|M| + Bk_F^2 = 0$. *Middle panel:* Normal band structure (thin quantum well) with no block mixing. *Right panel:* Inverted band structure with block mixing, characterized by $l_\Delta = (D\tau_\Delta)^{1/2}$ and $l_{SO} = (D\tau_{SO})^{1/2}$ (dash-dotted), assuming $\tau_\Delta < \tau_{SO}$. The energies $E_F = E_1 \dots E_5$ (from bottom to top) mark different horizontal cross-sections of the “phase-diagram” corresponding to the patterns 2O \rightarrow 1Sp, 2O \rightarrow 2U \rightarrow 1Sp, 2U \rightarrow 1Sp, 2Sp \rightarrow 2U \rightarrow 1Sp, and 2Sp \rightarrow 1Sp, respectively, that appear with increasing L . The magnetoresistance curves corresponding to these energies are shown schematically in Fig. 2. The diagram for the case of normal band structure with the block mixing is qualitatively similar.

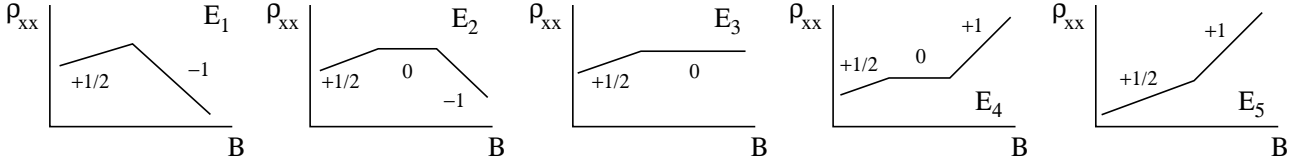


FIG. 2: Schematic view of the magnetoresistance curves $\rho_{xx}(B)$ in linear-logarithmic scale. Panels correspond to energies $E_1 \dots E_5$ from the right panel of Fig. 1 (inverted band structure). The numbers indicate the prefactor $\alpha = (\pi h/e^2)\partial\sigma/\partial\tau_H$ (here $\tau_H = L_H^2/D$) of the logarithmic magnetoresistance in different domains of magnetic field. For the purpose of visualization, the crossover regions (where τ_H is of the order of the corresponding symmetry-breaking time) are shown as cusps.

behaves as a single copy of symplectic class (1Sp) in the whole diffusive regime (ordinary WAL).

In the cases (i) and (ii), the magnetoresistance changes from positive to negative with increasing magnetic field. In the third case, the magnetoresistance is always positive in the diffusive regime.

IV. DISCUSSION AND CONCLUSIONS

To summarize, we have explored symmetries of the Bernevig-Hughes-Zhang Hamiltonian of 2D charge carriers in HgTe/HgCdTe quantum wells in the presence of physically relevant symmetry breaking perturbations. We have identified regimes of different symmetry in the parameter space and evaluated the corresponding quantum interference corrections to conductivity. Possible

regimes include 2O, 2U, 2Sp, and 1Sp, with the temperature dependence of the 2D weak (anti-)localization correction given by $\delta\sigma = \alpha(e^2/\pi h)\ln\tau_\phi(T)$, where $\alpha = -1, 0, 1$, and $1/2$, respectively. These regimes are summarized in Fig. 1.

Experimentally, the quantum interference—weak localization or antilocalization—shows up most directly in the transverse-field magnetoresistance. In particularly interesting situations, a symmetry breaking pattern then determines a succession of regions of magnetic field with different signs and/or prefactors of the weak localization magnetoresistance (see Fig. 2).

Let us now discuss published experimental data^{19,20} in context of our findings. In these papers the weak localization was studied in structures with both normal²⁰ and inverted^{19,20} band gaps. In both cases the authors observed weak positive magnetoresistance in low magnetic fields B which could be clearly attributed to WAL.

In higher fields, a crossover to negative magnetoresistance was observed that could be presumably attributed to weak localization. This corresponds to the $2\text{O} \rightarrow 1\text{Sp}$ symmetry pattern [characteristic for systems with relatively small carrier concentration, $E_F \ll m(k_F)$] in our terminology. The coefficient in front of $(e^2/\pi h) \ln \tau_H$ (where $\tau_H = L_H^2/D$) was found to be consistent with $1/2$, as expected for the 1Sp regime.

More experimental work is clearly needed to explore systematically different parameter regimes with different types of quantum interference behavior. We hope that our paper will stimulate such experimental activity and will be helpful in identification of different regimes and analysis of quantum interference contributions to conductivity.

When this manuscript was in preparation, we learned about preprints Ref. 25,26 with partly overlapping content.

V. ACKNOWLEDGMENTS

We are grateful C. Brüne, M. Dyakonov, A. Germanenko, E. Hankiewicz, V. Kachorovskii, G. Minkov, L. Molenkamp, S. Tarasenko, and G. Tkachov for numerous illuminating discussions. This work was supported by BMBF, DFG-RFBR, DFG-SPP “Semiconductor spintronics”, and DFG-CFN. P.M.O. and A.D.M. acknowledge the hospitality of Kavli Institute of Theoretical Physics of University of California, Santa Barbara, where a part of this work was done.

Appendix A: Boundary scattering

In this Appendix we consider the properties of the BHZ Hamiltonian with the boundary condition $\psi = 0$, see Sec. II C. We demonstrate that the symplectic (block-wise) time-reversal symmetry is strongly violated by this boundary condition.

Consider the upper block of the BHZ Hamiltonian (to minimize the notation we assume $A = 1$)

$$h = \begin{pmatrix} M - B\mathbf{k}^2 & k_x - ik_y \\ k_x + ik_y & -M + B\mathbf{k}^2 \end{pmatrix}. \quad (\text{A1})$$

At energy $E = |\mathbf{k}| = \sqrt{M/B}$, diagonal elements of the Hamiltonian vanish leading to the emergence of symplectic time-reversal symmetry. There are two plain wave solutions at this energy with the fixed momentum k_x along x direction:

$$\psi_{\pm} = \begin{pmatrix} 1 \\ a_{\pm} \end{pmatrix} e^{ik_x x \pm i\sqrt{E^2 - k_x^2} y}, \quad (\text{A2})$$

$$a_{\pm} = \frac{k_x \pm i\sqrt{E^2 - k_x^2}}{E}. \quad (\text{A3})$$

These two states are related by the time-reversal operation:

$$\sigma_y \psi_{\pm}^*(k_x) = -ia_{\mp} \psi_{\mp}(-k_x). \quad (\text{A4})$$

Assume a semi-infinite plane $y > 0$ with the hard wall boundary at $y = 0$. The eigenstate of the boundary problem will contain both the incident wave ψ_- and reflected wave ψ_+ with some amplitudes. In order to fulfill the boundary condition $\psi|_{y=0} = 0$, we have to add a third eigenfunction of the 2D problem exponentially decaying in the bulk $y > 0$. This solution has the form

$$\psi_0 = \begin{pmatrix} 1 \\ a_0 \end{pmatrix} e^{ik_x x - \sqrt{1 - B^2(E^2 - k_x^2)} y/B}, \quad (\text{A5})$$

$$a_0 = \frac{Bk_x - \sqrt{1 - B^2(E^2 - k_x^2)}}{1 + BE}. \quad (\text{A6})$$

The scattering state can now be directly constructed:

$$\psi = \psi_- + r \psi_+ + r_0 \psi_0, \quad (\text{A7})$$

$$r = \frac{a_- - a_0}{a_0 - a_+}, \quad r_0 = \frac{a_+ - a_-}{a_0 - a_+}. \quad (\text{A8})$$

Far from the boundary, the solution ψ_0 decays and the factor r yields the reflection amplitude.

If the boundary condition preserve time-reversal symmetry, the following state would be another legitimate solution of the boundary problem at $y \rightarrow +\infty$:

$$\sigma_y \psi^* = \sigma_y (\psi_- + r \psi_+)^*. \quad (\text{A9})$$

Applying relations (A4), we obtain

$$\begin{aligned} \sigma_y \psi^* &= \sigma_y \psi_-^* + r^* \sigma_y \psi_+^* \\ &= -ia_+ \psi_+(-k_x) - ia_- r^* \psi_-(-k_x) \\ &= -ia_- r^* \left[\psi_-(-k_x) + \frac{a_+}{a_- r^*} \psi_+(-k_x) \right]. \end{aligned} \quad (\text{A10})$$

Now we compare the prefactor in front of $\psi_+(-k_x)$ with the reflection amplitude at $-k_x$. This will indicate the degree of time-reversal symmetry breaking during one scattering off the boundary. Actually, the following identity holds:

$$\frac{a_+}{a_- r^*(k_x)} = -r(-k_x). \quad (\text{A11})$$

The sign here is just opposite to what one would expect from the time-reversal invariance. Thus the symmetry is maximally violated.

Appendix B: Relativistic corrections at the bottom of the band

At energies close to the bottom of the band, such that $E = M + \epsilon$ with $\epsilon \ll M$, the BHZ Hamiltonian acquires an approximate orthogonal time-reversal symmetry, see Sec. III B. It is related to the fact that the spin

of the electron is almost aligned with the z axis and very weakly depends on the momentum. The Hamiltonian can be approximated as $h \approx \mathbf{k}^2/2M$ (in this Appendix we assume $A = 1$ and $B = 0$) up to small relativistic corrections. The situation is completely analogous to the non-relativistic Schrödinger approximation to the Dirac Hamiltonian. Below we derive these relativistic corrections for the upper block of Eq. (2).

Let us write explicitly the two-component Dirac equation with an external potential V :

$$(M + V)u + k_-v = (M + \epsilon)u, \quad (\text{B1})$$

$$k_+u - (M - V)v = (M + \epsilon)v. \quad (\text{B2})$$

Here $k_{\pm} = k_x \pm ik_y$. We now express v from the second equation,

$$v = (2M + \epsilon - V)^{-1}k_+u, \quad (\text{B3})$$

and use it to obtain a single second order equation for the component u ,

$$[V + k_-(2M + Bk^2 + \epsilon - V)^{-1}k_+]u = \epsilon u. \quad (\text{B4})$$

In order to recast it in the form of an equivalent one-component Schrödinger equation, we have to correct the normalization of the wave function. The initial spinor function is normalized according to $|u|^2 + |v|^2 = 1$. We rescale the component u as

$$u = \left(1 - \frac{k^2}{8M^2}\right)\phi. \quad (\text{B5})$$

With the help of Eq. (B3), this yields $|\phi|^2 = 1 + O(k^4)$. We now substitute u from Eq. (B5) into Eq. (B4) and

expand in powers of k . In order to cancel the terms $\sim \epsilon k^2$ we have to multiply both sides of Eq. (B4) by $(1 - k^2/8M^2)$. This finally yields the Schrödinger equation $h\phi = \epsilon\phi$ with the Hamiltonian

$$h = \frac{k^2}{2M} - \frac{k^4}{8M^3} + V + \frac{k_-Vk_+}{4M^2} - \frac{k^2V + Vk^2}{8M^2}. \quad (\text{B6})$$

First two terms represent the expansion of the relativistic dispersion relation $\epsilon = \sqrt{M^2 + k^2} - M$ in powers of k . The last three terms appear due to external potential V . In an analogous calculation for the full 4D Dirac Hamiltonian, the last two terms of the Hamiltonian would correspond to spin-orbit scattering. In our 2D case, non-relativistic wave function is just the scalar ϕ without any spin structure. The ‘‘spin-orbit’’ scattering in this case can be rewritten as the interaction with a fictitious magnetic field. Let us introduce the vector potential according to

$$a_x = -\frac{\nabla_y V}{4eM}, \quad a_y = \frac{\nabla_x V}{4eM}. \quad (\text{B7})$$

This allows us to represent the Hamiltonian as

$$h = \frac{(\mathbf{k} - e\mathbf{a})^2}{2M} - \frac{k^4}{8M^3} + V - \frac{e^2\mathbf{a}^2}{2M} - \frac{eb}{2M}. \quad (\text{B8})$$

The effective magnetic field

$$b = \frac{\nabla^2 V}{4eM}$$

leads to breaking of the approximate ‘‘orthogonal’’ time-reversal symmetry with the rate $1/\tau_A$ as calculated in Sec. III B, see Eqs. (60)-(62).

¹ A. H. Castro Neto, F. Guinea, N. M. R. Peres, K. S. Novoselov, and A. K. Geim, *Rev. Mod. Phys.* **81**, 109 (2009).
² K. S. Novoselov *Rev. Mod. Phys.* **83**, 837 (2011); Andre K. Geim, *ibid* 851 (2011).
³ M. Z. Hasan and C. L. Kane, *Rev. Mod. Phys.* **82**, 3045 (2010).
⁴ X.-L. Qi and S.-C. Zhang, *Rev. Mod. Phys.* **83**, 1057 (2011).
⁵ B.A. Bernevig, T.L. Hughes, and S.-C. Zhang, *Science* **314**, 1757 (2006).
⁶ M. König, S. Wiedmann, C. Brüne, A. Roth, H. Buhmann, L.W. Molenkamp, X.-L. Qi, and S.-C. Zhang, *Science* **318**, 766 (2007).
⁷ C. L. Kane and E. J. Mele, *Phys. Rev. Lett.* **95**, 146802 (2005); *ibid.* **95**, 226801 (2005).
⁸ L. Fu and C. L. Kane, *Phys. Rev. B* **76**, 045302 (2007); L. Fu, C.L. Kane, and E.J. Mele, *Phys. Rev. Lett.* **98**, 106803 (2008).
⁹ D. Hsieh, D. Qian, L. Wray, Y. Xia, Y.S.Hor, R.J. Cava, and M.Z.Hasan, *Nature* **452**, 7190 (2008).
¹⁰ M. König, H. Buhmann, L.W. Molenkamp, T. Hughes, C.-

X. Liu, X.-L. Qi, and S.-C. Zhang, *J. Phys. Soc. Jpn.* **77**, 031007 (2008); A. Roth, C. Brüne, H. Buhmann, L.W. Molenkamp, J. Maciejko, X.-L. Qi, and S.-C. Zhang, *Science* **325**, 294 (2009).
¹¹ P. M. Ostrovsky, I. V. Gornyi, and A. D. Mirlin, *Phys. Rev. Lett.* **105**, 036803 (2010).
¹² C. Liu, T.L. Hughes, X.-L. Qi, K. Wang, and S.-C. Zhang, *Phys. Rev. Lett.* **100**, 236601 (2008).
¹³ D.G. Rothe, R.W. Reintaler, C.-X. Liu, L.W. Molenkamp, S.-C. Zhang, and E.M. Hankiewicz, *New J. Phys.* **12** 065012 (2010).
¹⁴ G. Tkachov and E. M. Hankiewicz, *Phys. Rev. B* **84**, 035444 (2011).
¹⁵ R. Winkler, *Spin-Orbit Coupling Effects in Two-Dimensional Electron and Hole Systems*, Springer Tracts in Modern Physics, Volume 191, (Springer, Berlin, 2003).
¹⁶ P.M. Ostrovsky, I.V. Gornyi, and A.D. Mirlin, *Phys. Rev. B* **74**, 235443 (2006).
¹⁷ V.Yu. Kachorovskii *et al.*, unpublished.
¹⁸ S. Hikami, A. I. Larkin, and Y. Nagaoka, *Prog. Theor. Phys.* **63**, 707 (1980).
¹⁹ G.M. Minkov, A.V. Germanenko, O.E. Rut, A.A.

Sherstobitov, S.A. Dvoretzki, and N.N. Mikhailov, arXiv:1202.1093.

²⁰ E.B. Olshanetsky, Z.D. Kvon, G.M. Gusev, N.N. Mikhailov, S.A. Dvoretzki, and J.C. Portal, JETP Letters **91**, 347 (2010).

²¹ C. Brüne *et al.*, unpublished.

²² E. McCann, K. Kechedzhi, V.I. Fal'ko, H. Suzuura, T. Ando, and B.L. Altshuler, Phys. Rev. Lett. **97**, 146805 (2006); K. Kechedzhi, E. McCann, V.I. Fal'ko, H. Suzuura, T. Ando, and B. L. Altshuler, Eur. Phys. J. Special Topics **148**, 39-54 (2007).

²³ M.O. Nestoklon, N.S. Averkiev, and S.A. Tarasenko, Solid State Comm. **151**, 1550 (2011).

²⁴ The term

$$\ln \left(\frac{\tau}{\tau_\phi} + \frac{\tau}{\tau_{SO}} + \frac{\tau}{\tau_A + \tau_\Delta} \right)$$

corresponding to the pair of symmetries T_{xx} and T_{yy} is written in the form that describes correctly all the asymp-

otics and crossovers, except possibly for the “triple point” $\min[\tau_\phi, \tau_{SO}] \sim \tau_A \sim \tau_\Delta$, when both T_{xx} and T_{yy} symmetries are broken on the same scale. Note that this term contains a sum of symmetry-breaking times (not rates). With the same accuracy one can use an alternative (less compact) expression

$$\begin{aligned} & \ln \left(\frac{\tau}{\tau_\phi} + \frac{\tau}{\tau_{SO}} + \frac{\tau}{\tau_A} \right) + \ln \left(\frac{\tau}{\tau_\phi} + \frac{\tau}{\tau_{SO}} + \frac{\tau}{\tau_\Delta} \right) \\ & - \ln \left(\frac{\tau}{\tau_\phi} + \frac{\tau}{\tau_{SO}} + \frac{\tau}{\tau_A} + \frac{\tau}{\tau_\Delta} \right) \end{aligned}$$

which contains a sum of symmetry-breaking rates. In order to rigorously describe the above “triple-point crossover”, one should perform a microscopic calculation.

²⁵ I. Garate and L. Glazman, arXiv:1206.1239.

²⁶ V. Krueckl and K. Richter, arXiv:1207.1294.